Green Intelligent Systems and Applications

Research Article
Volume 5(2), 2025, 140–149
https://doi.org/10.53623/gisa.v5i2.761

Design and Build a Push-Pull Inverter for Room Lighting

Munnik Haryanti[1]*, Bekti Yulianti[1], Cynthia Rahmawati[2], Iwan Adhicandra[3]

[1]Electrical Engineering Study Program, Dirgantara Marsekal Suryadarma University, Jakarta, Indonesia
[2]Aeronautical Engineering Study Program, Dirgantara Marsekal Suryadarma University, Jakarta, Indonesia
[3]Informatics Engineering Study Program, Bakrie University, Jakarta, Indonesia

*Correspondence: munnik@unsurya.ac.id

SUBMITTED: 7 July 2025; REVISED: 2 August 2025; ACCEPTED: 4 August 2025

ABSTRACT: This study addressed the issue of harmonic distortion in solar power systems that required inverters to convert DC voltage to AC for indoor lighting applications. The objective was to design and evaluate a push-pull inverter incorporating pulse width modulation (PWM) to reduce harmonics and ensure a stable voltage output. A push-pull topology was selected because of its relatively simple design and ability to step up DC voltage using a transformer, making it suitable for low- to medium-power applications. The inverter employed two metal–oxide–semiconductor field-effect transistor (MOSFET) switching devices operated alternately to generate AC waves at the output. The core of the design was a 50 Hz pulse generator producing a 5 V pulse signal with a small current, which was then amplified using a current amplifier before being supplied to the transformer. The transformer functioned to induce the electromagnetic field from the pulse source and release it at a higher voltage of 220 V. Experimental testing was performed using 2.3 W, 5 W, and 8 W LED lights. A minor modification to the gate resistor improved system performance, resulting in stable transformer output voltages at 5 W and 8 W loads. These results demonstrated that the PWM-controlled push-pull inverter successfully reduced harmonics and maintained voltage stability under higher loads, making it effective for indoor LED lighting powered by solar energy. Future studies could aim to enhance efficiency at lower loads, minimize switching losses, and implement more advanced PWM techniques to achieve performance levels comparable to pure sine wave inverters.

KEYWORDS: Push-pull inverter; solar panel; PWM technique; transformer; MOSFET

1. Introduction

Inverters are critical components in modern power conversion systems, enabling the transformation of direct current (DC) into alternating current (AC) to support the operation of devices that require AC supply. Based on output waveform characteristics, inverters are typically categorized as square wave (push-pull), modified sine wave, or pure sine wave types [1]. Square wave or push-pull inverters generate rectangular output waveforms suitable for applications where waveform quality is less critical. Modified sine wave inverters produce stepped approximations of sinusoidal signals, while pure sine wave inverters deliver high-quality AC outputs that closely resemble grid-supplied sine waves [2]. These technologies are widely deployed in solar energy systems, uninterruptible power supplies (UPS), automotive

power converters, and a variety of electronic devices [3].

Among these options, push-pull inverters have gained prominence in low- to medium-power applications due to their simple topology, cost-effectiveness, and ability to step up DC voltages using transformers [4]. Such characteristics make them attractive for solar-powered lighting, portable power systems, and small-scale residential or industrial loads. Despite these advantages, push-pull inverters often suffer from substantial harmonic distortion in their output waveforms [5]. Excessive harmonics reduce conversion efficiency, degrade power quality, and may shorten the operational life of connected devices, making waveform improvement a crucial design challenge.

PWM is widely recognized as an effective strategy to mitigate harmonic distortion while maintaining stable voltage levels. By varying pulse widths at constant frequency and amplitude, PWM enables improved control of output voltage, power delivery, and waveform quality [1]. Bipolar switching, wherein pulses alternate between positive and negative voltages, offers an efficient means of producing AC outputs with reduced harmonics [6]. Although PWM techniques have been extensively studied, their application in small-scale push-pull inverters designed specifically for indoor LED lighting particularly in solar-powered systems, remains limited. Addressing this gap is essential because indoor lighting applications demand consistent voltage regulation and low harmonic distortion to ensure optimal efficiency and extended device lifespan.

This study hypothesized that integrating bipolar PWM control into a MOSFET-based push-pull inverter would significantly reduce harmonic distortion while maintaining stable output voltage across varying LED loads. To test this hypothesis, a push-pull inverter was designed using two MOSFET switches operating alternately to generate AC waveforms. A 50 Hz pulse generator served as the control core, producing a 5 V signal with minimal current, which was subsequently amplified before being supplied to a transformer that stepped up the voltage to 220 V. The proposed configuration aimed to combine simplicity and cost-efficiency with improved waveform quality, making it well-suited for small-scale solar lighting systems.

The significance of this work lies in its potential to advance the design of affordable and efficient inverters for off-grid and portable applications. By enhancing voltage stability and reducing harmonics in low-power systems, the findings contribute to the broader goal of improving the reliability and performance of renewable energy technologies. The primary aim of this study was therefore to design, construct, and experimentally evaluate a PWM-controlled push-pull inverter for indoor LED lighting. Performance was assessed under 2.3 W, 5 W, and 8 W loads to determine whether the proposed approach could deliver stable voltage and improved waveform quality, thereby providing a feasible solution for small-scale solar power applications.

2. Materials and Methods

2.1. System design overview.

The design process began with the development of a comprehensive block diagram for the push-pull inverter (Figure 1), which served as the foundation for both simulation and hardware implementation. A literature review was first conducted to explore theories related to inverter operation, PWM strategies, and control techniques, as well as to identify the limitations of existing designs. Relevant software tools were also evaluated to support schematic design,

simulation, and signal analysis. Once the theoretical framework was established, the circuit design phase commenced. The pulse signal generator and current amplifier were developed using Eagle and EasyEDA, which allowed precise PCB layout and component selection. Network simulations were then carried out using SPICE-based simulators and EWM Workbench to model the inverter's electrical behavior, including voltage waveform quality and switching characteristics. These simulations helped optimize component values and identify potential issues before physical assembly. To control the inverter, a microcontroller was programmed to generate 50 Hz PWM signals with appropriate duty cycles, enabling efficient operation of the MOSFET switches [7]. Finally, experimental testing was planned to validate the system once all components were integrated, ensuring that the design met the intended performance specifications under realistic load conditions [8].

Figure 1. Block diagram of the inverter design.

2.2. Pulse signal generation and voltage amplification.

The core of the inverter design was a 50 Hz pulse generator, which served as the primary control unit for driving the transformer (Figure 2). An Arduino microcontroller was used to implement this function, utilizing Timer 0 to produce a stable square-wave signal. The microcontroller generated a 5 V pulse with low current, sufficient for control but inadequate to directly drive the transformer. To address this limitation, a current amplifier stage was introduced to boost the signal to the required current levels, ensuring efficient switching of the MOSFETs and reliable transformer operation. The amplified pulses alternated at a fixed frequency, creating the magnetic flux necessary to energize the transformer core. Through electromagnetic induction, the transformer stepped up the input voltage to 220 V at the output. This configuration enabled the system to convert low-voltage DC into an AC signal suitable for powering indoor lighting and other low-power applications [9].

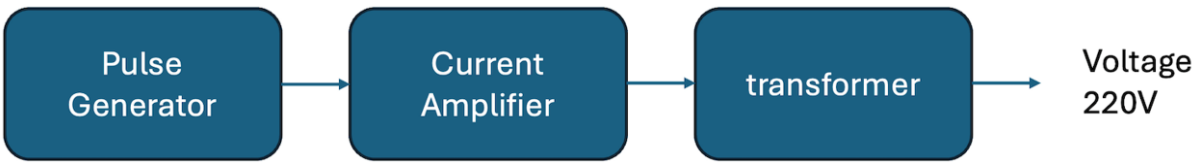

Figure 2. Block diagram of the pulse signal inverter system.

2.3. Operating principle of the box signal inverter.

The working principle of the inverter is illustrated in Figure 3. The system operated by injecting two box wave signals, labeled A and B, into the primary winding of an iron-core transformer. These signals were generated with a 180° phase difference, ensuring that when one signal was at a positive voltage, the other was at a negative voltage. This arrangement created a bidirectional flow of current in the primary coil, effectively producing an alternating magnetic field in the transformer core. As the magnetic field alternated, electromagnetic induction occurred, energizing the secondary winding of the transformer [10]. This process stepped up the voltage from the low-level DC input to a higher AC output, represented as signal C. To

control this operation, four MOSFET switches were arranged in an H-Bridge configuration, allowing precise switching between positive and negative voltage states. Each MOSFET gate such as HOA, HOB, LOA, and LOB, was uniquely labeled to simplify signal monitoring and troubleshooting during simulation and experimental testing. This configuration not only enabled efficient conversion of DC to AC but also provided flexibility in waveform generation, making the inverter suitable for low- to medium-power applications such as solar-powered indoor lighting [11].

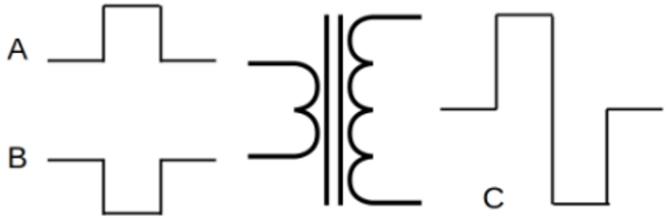

Figure 3. Operating principle of the box signal inverter: A and B (the input square wave signal consist of two square waves with a 180^0 phase different), and C (output signal voltage).

3. Results and Discussion

3.1. Effect of gate resistor on transformer output.

The performance of the inverter was first evaluated using an H-Bridge configuration (Figure 4) to analyze the effect of different gate resistor values on output voltage stability. Three sets of experiments were conducted: with 1 kΩ, 500 Ω, and 300 Ω gate resistors, as summarized in Tables 1–3. With a 1 kΩ resistor (Table 1), the output voltage remained stable at 233 V for no load and 0.8 W load, but dropped significantly to 160 V at 2.3 W.

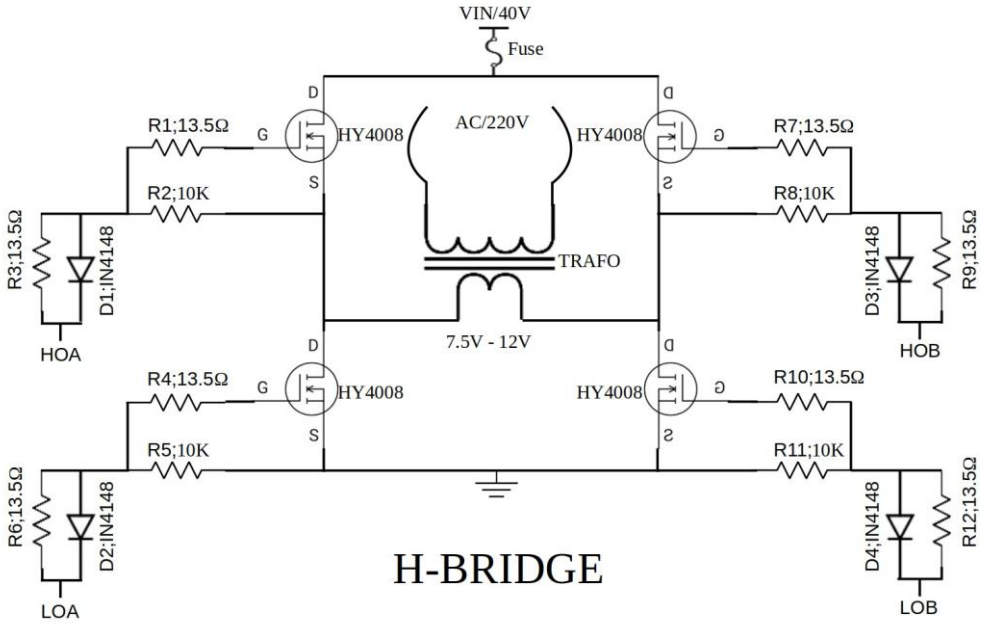

Figure 4. H-Bridge configuration of the inverter.

This reduction was attributed to insufficient gate drive voltage, which limited the MOSFET's ability to conduct fully, thereby reducing transformer induction current. Reducing the gate resistor to 500 Ω (Table 2) improved performance, with the 2.3 W load reaching 190

V. Further decreasing the resistor to 300 Ω (Table 3) increased the 2.3 W load voltage to 210 V, approaching the desired 220 V. These results indicate that optimizing the gate resistor value enhances MOSFET switching performance by delivering stronger gate drive signals, thereby increasing transformer excitation. For long-term stability, voltage regulation at the gate input is recommended [12]. An adjustable regulator such as IC LM2576, capable of supplying higher gate currents, could further stabilize the inverter output.

Table 1. Load test results with 1 kΩ gate resistor.

Condition	Current	Input transformer voltage	Output transformer voltage
No load	0.162	8.16	233
0.8 watt load	0.178	8.16	233
Load 2.3 watts	0.577	7	160

Table 2. Load test results with 500 Ω gate resistor.

Condition	Current	Input transformer voltage	Output transformer voltage
No load	0.2	8.8	243
0.8 watt load	-	-	-
Load 2.3 watts	0.51	7.8	190

Table 3. Load test results with 300 Ω gate resistor.

Condition	Current	Input transformer voltage	Output transformer voltage
No load	0.29	9.4	256
0.8 watt load	-	-	-
Load 2.3 watts	0.56	8.5	210

3.2. Performance under higher loads.

The inverter was further tested with 5 W and 8 W LED loads to assess behavior at higher power levels (Figure 5). Without load, the inverter produced an AC voltage of 253 V. When powering a 5 W LED lamp, the voltage dropped to 208 V, and for an 8 W LED lamp, it decreased to 200 V. Although the output voltage declined with increasing load, it remained within an acceptable range for low-power lighting applications. The source power was supplied by a solar panel array delivering an average voltage of 36–38 V with a maximum power of 1200 W. A 15 A fuse was integrated at the input line to protect the system against short circuits or overloads, ensuring operational safety. These results demonstrate that the inverter could reliably power small indoor lighting systems, though further optimization of gate control and transformer design may be required to achieve consistent 220 V output across all loads. Adjustments to the PWM duty cycle or incorporating feedback control could also improve voltage regulation for larger loads [13, 14].

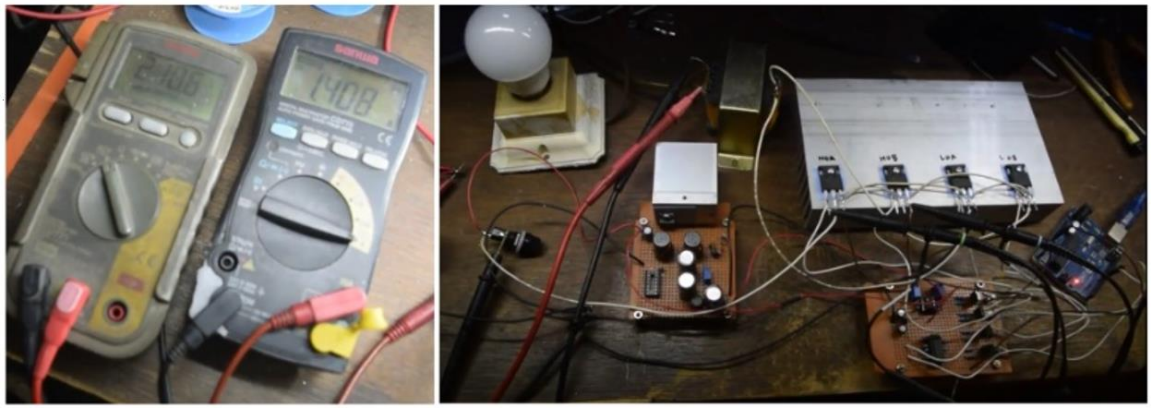

Figure 5. Inverter tested with 5 W and 8 W LED loads.

3.3. Output signal characteristics.

To better understand waveform behavior, inverter output signals were captured under multiple experimental conditions, as shown in Figure 6(A–C). The box wave signals generated by the push-pull configuration exhibited clear phase alternation, essential for producing the desired AC waveform. However, minor waveform distortions were observed under higher loads, indicating residual harmonic components. These distortions were consistent with the voltage drops recorded in Tables 1–3 and were primarily caused by insufficient MOSFET gate drive and transformer saturation effects at higher currents. The results suggest that while the inverter successfully produced an alternating output, further refinement of PWM control and component selection is necessary to improve waveform purity. Using faster-switching MOSFETs and optimizing the transformer core material could reduce harmonics, while advanced PWM techniques such as sinusoidal PWM might produce smoother waveforms. These improvements would enhance the inverter's suitability for sensitive electronic devices while maintaining its effectiveness for lighting applications [15, 16].

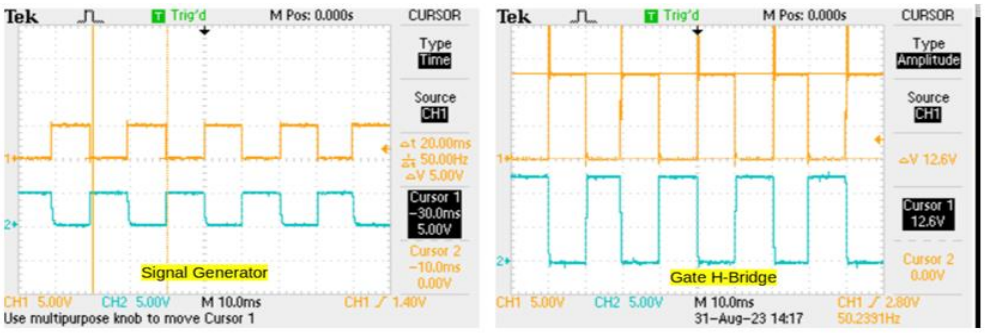

(A)

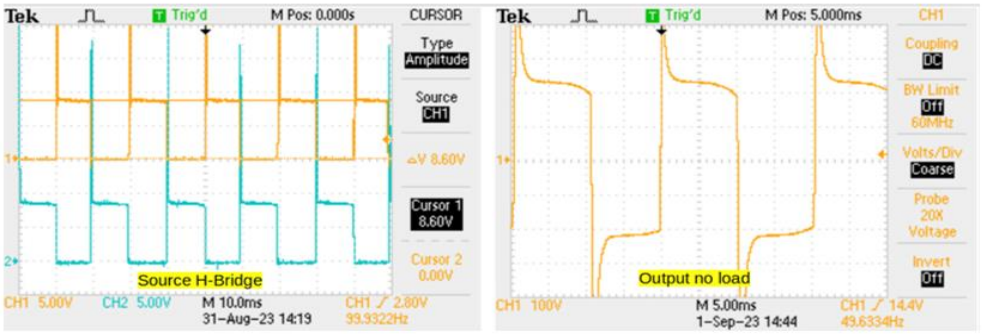

(B)

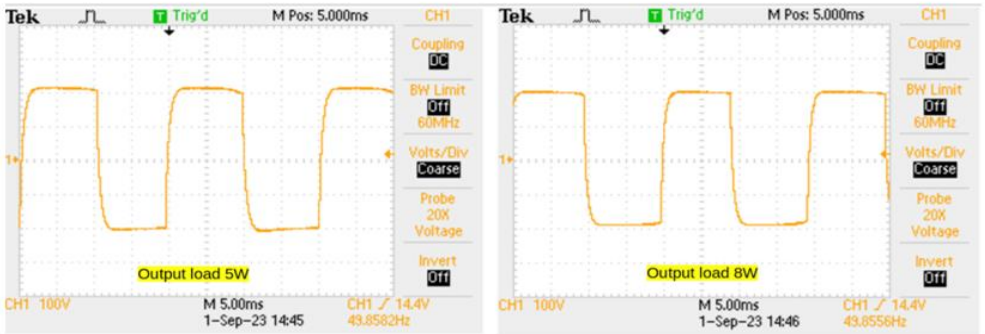

(C)

Figure 6. Inverter output waveforms under different test conditions: (A) no load, (B) 5 W load, and (C) 8 W load.

3.4. Effect of resistor variation on inverter performance.

The inverter was tested under various load conditions (2.3 W, 5 W, and 8 W) while varying resistor values at the transistor base, diode, and MOSFET gate to determine their impact on performance. The results are summarized in Table 4. Initial experiments showed that sufficient voltage and current at the MOSFET gate were critical for driving higher loads effectively. Using a 13.5 Ω resistor on the gate leg significantly improved current delivery, allowing the inverter to provide more stable output voltages for both 5 W and 8 W loads. Without this adjustment, the MOSFETs could not fully switch on, resulting in voltage drops and unstable operation. With the optimized resistor configuration, the inverter achieved an average efficiency of 30%, calculated as the output power minus no-load dissipation divided by the input power. Although efficiency remained modest due to switching losses and transformer limitations, this improvement demonstrated the importance of proper gate drive design for small-scale push-pull inverters [17, 18].

Table 4. Results of multiple load experiments with Rbase 470 Ω, Rdiode 13.5 Ω, and Rgate 13.5 Ω.

Condition	Current (A)	Input power (W)	Output transformer voltage (Vac)	Efficiency %
No load	0.9	32.4	253	-
5 Watt Load	1.36	48.96	208	30.2
8 Watt Load	1.85	66.6	198	23.3

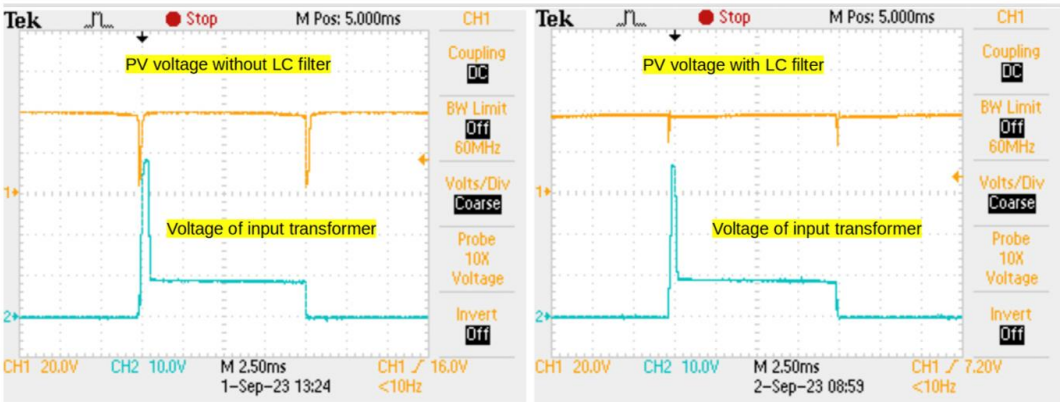

Figure 7. Comparison of PV voltage without and with filter.

3.5. Impact of LC filtering on DC-DC converter.

During testing, an audible noise was observed in the DC-DC converter, prompting further investigation. Measurements revealed a 100 Hz voltage ripple at the solar panel input (Figure 8), caused by switching effects in the MOSFETs that demanded substantial power to drive the step-up transformer. To mitigate this issue, an LC filter was introduced, consisting of nine turns of 1 mm diameter wire and a 10,000 µF/50 V capacitor, as shown in Figure 8. The addition of the LC filter reduced the ripple amplitude by more than half (Figure 7), resulting in a noticeable reduction in audible noise, though some residual sound persisted. Performance results with the LC filter are summarized in Table 5. While the filter slightly increased no-load current consumption (from 0.9 A to 1.5 A), efficiency improved to an average of 34%. At a 5 W load, the inverter output stabilized at 212 V, whereas at 8 W the voltage dropped to 180 V, reflecting limitations in transformer capability under higher loads. Overall, the LC filter enhanced power quality and efficiency, providing a valuable improvement for solar-powered inverter

applications, though further optimization of the transformer and MOSFET drive circuitry is recommended [16, 19, 20].

Table 5. Results of multiple load experiments with LC filter on PV lines.

Condition	Current (A)	Input power (W)	Output transformer voltage (Vac)	Efficiency %
No load	1.5	54	259	-
5 Watt Load	1.9	68.4	212	34.7
8 Watt Load	2.3	82.8	180	27.7

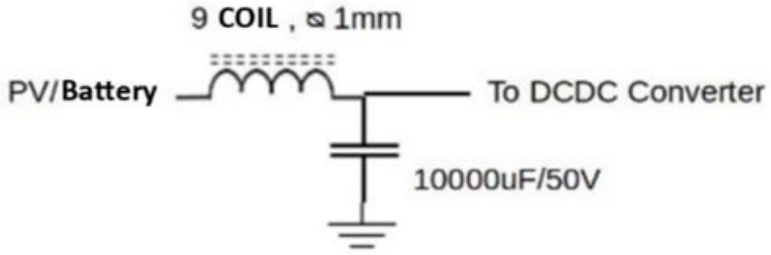

Figure 8. LC filter on DC-DC converter circuit.

4. Conclusions

This study successfully designed and tested a square wave push-pull inverter using 2.3 W, 5 W, and 8 W LED loads. The results showed that the transformer output voltage remained stable for 5 W and 8 W loads after optimizing the MOSFET gate drive by reducing the gate resistor value. The initial voltage drops were caused by insufficient gate input voltage, which limited the MOSFET conduction and reduced the induced current in the transformer. Adjusting the gate resistor improved switching performance, increased FET output voltage, and allowed greater transformer excitation. When integrated with a solar panel as part of a renewable energy system, the inverter operated with a measured heatsink temperature of approximately 50 °C. Without an LC filter, significant voltage ripple appeared on the DC input line, causing audible noise in the DC-DC converter and limiting efficiency to around 30%, with a no-load dissipation of 32.4 W. The addition of an LC filter effectively reduced ripple amplitude and noise while improving overall efficiency to approximately 34%. These findings demonstrate that proper gate drive design and input filtering are critical for enhancing the stability, efficiency, and power quality of small-scale inverters for solar-powered applications. Future work should focus on advanced PWM control and transformer optimization to achieve higher efficiency and better waveform quality.

Acknowledgments

This research was funded by the Institute for Research and Community Service, Marsekal Suryadarma Aerospace University, in 2023 under Contract No. 21/P-I/LP2M/UNSURYA/XII/2024.

Author Contribution

The study was conceptualized by Munnik Haryanti, S.T., M.T. The methodology was developed by Munnik Haryanti, S.T., M.T., and Iwan Adhicandra, Ph.D. Data collection was carried out by Cynthia Rahmawati, S.Si., M.Si (Han), while data analysis was performed by Munnik Haryanti, S.T., M.T., and Bekti Yulianti, S.T., M.T. The manuscript was written by

Cynthia Rahmawati, S.Si., M.Si (Han). Supervision was provided by Iwan Adhicandra, Ph.D., and Munnik Haryanti, S.T., M.T. Funding for the research was secured by Munnik Haryanti, S.T., M.T., and Iwan Adhicandra, Ph.D.

Competing Interest

The authors declare that they have no known competing financial interests or personal relationships that could have appeared to influence the work reported in this article.

References

[1] Rymarski, Z.; Ptak, P. (2025). Special Issue: New Technologies for Power Electronic Converters and Inverters. *Applied Sciences*, *15*, 5753. https://doi.org/10.3390/app15105753.

[2] Kjaer, S.B.; Blaabjerg, F. (2003). Design optimization of a single phase inverter for photovoltaic applications. Proceedings of the IEEE 34th Annual Conference on Power Electronics Specialist (PESC'03), Acapulco, Mexico, 15–19 June 2003; IEEE: Piscataway, NJ, USA; pp. 1183–1190.

[3] Fan, L.; Miao, Z. (2023). Modeling and Stability Analysis of Inverter-Based Resources, 1st ed.; CRC Press: Boca Raton, USA.

[4] Kanagachidambaresan, G.R. (2021). Introduction to KiCad design for breakout and circuit designs. In Role of Single Board Computers (SBCs) in Rapid IoT Prototyping; Springer: Cham, Switzerland; pp. 165–175.

[5] Zhang, S.; Li, H.; Liu, Y.; Liu, X.; Lv, Q.; Du, X.; Zhang, J. (2024). An improved SPWM strategy for effectively reducing total harmonic distortion. *Electronics*, *13*, 3326. https://doi.org/10.3390/electronics13163326.

[6] Ashraf, N.; Abbas, G.; Ullah, N.; Otaibi, S.A.; Althobaiti, A.; Zubair, M.; Farooq, U. (2021). A bipolar voltage gain boost AC-AC converter based on four switching transistors. *Applied Sciences*, *11*, 10254. https://doi.org/10.3390/app112110254.

[7] Merenda, M.; Iero, D.; Pangallo, G.; Falduto, P.; Adinolfi, G.; Merola, A.; Graditi, G.; Della Corte, F.G. (2019). Open-source hardware platforms for smart converters with cloud connectivity. *Electronics*, *8*, 367. https://doi.org/10.3390/electronics8030367.

[8] Mastouri, H.; Ennawaoui, A.; Remaidi, M.; Sabani, E.; Derraz, M.; El Hadraoui, H.; Ennawaoui, C. (2025). Design, modeling, and experimental validation of a hybrid piezoelectric–magnetoelectric energy-harvesting system for vehicle suspensions. *World Electric Vehicle Journal*, *16*, 237. https://doi.org/10.3390/wevj16040237.

[9] Zdiri, M.A.; Dhouib, B.; Alaas, Z.; Hadj Abdallah, H. (2023). A low-voltage AC, low-voltage DC, and high-voltage DC power distribution system with grid: Design and analysis. *Applied Sciences*, *13*, 808. https://doi.org/10.3390/app13020808.

[10] Martín Sánchez, P.; Rodríguez Sánchez, F.J.; Santiso Gómez, E. (2020). An experimental strategy for characterizing inductive electromagnetic energy harvesters. *Sensors*, *20*, 647. https://doi.org/10.3390/s20030647.

[11] Awad, H.; Bayoumi, E.H.E. (2025). Next-generation smart inverters: Bridging AI, cybersecurity, and policy gaps for sustainable energy transition. *Technologies*, *13*, 136. https://doi.org/10.3390/technologies13040136.

[12] Huang, Z.; Du, Z.; Gao, J.; Zhong, G. (2025). Transient stability assessment of power systems based on temporal feature selection and LSTM-transformer variational fusion. *Electronics*, *14*, 2780. https://doi.org/10.3390/electronics14142780.

[13] Esenboğa, B.; Demirdelen, T. (2023). Soft-switching smart transformer design and application for photovoltaic integrated smart city power distribution. *Sustainability*, *15*, 32. https://doi.org/10.3390/su15010032.

[14] Rihar, A.; Nemec, M.; Lavrič, H.; Zajec, P.; Vončina, D.; Nedeljković, D.; Ambrožič, V.; Drobnič, K. (2024). Emerging technologies for advanced power electronics and machine design in electric drives. *Applied Sciences*, *14*, 11559. https://doi.org/10.3390/app142411559.

[15] Ginzburg-Ganz, E.; Baimel, D.; Belikov, J.; Levron, Y. (2025). Design and modeling guidelines for auxiliary voltage sensing windings in high-voltage transformers and isolated converters. *Electronics*, *14*, 1519. https://doi.org/10.3390/electronics14081519.

[16] Yao, W.; Lu, J.; Taghizadeh, F.; Bai, F.; Seagar, A. (2023). Integration of SiC devices and high-frequency transformer for high-power renewable energy applications. *Energies*, *16*, 1538. https://doi.org/10.3390/en16031538.

[17] Ivanovic, Z.; Knezic, M. (2022). Modeling push–pull converter for efficiency improvement. *Electronics*, *11*, 2713. https://doi.org/10.3390/electronics11172713.

[18] Meshael, H.; Elkhateb, A.; Best, R. (2023). Topologies and design characteristics of isolated high step-up DC–DC converters for photovoltaic systems. *Electronics*, *12*, 3913. https://doi.org/10.3390/electronics12183913.

[19] Dash, D.K.; Sadhu, P.K. (2023). A review on the use of active power filter for grid-connected renewable energy conversion systems. *Processes*, *11*, 1467. https://doi.org/10.3390/pr11051467.

[20] Arévalo, P.; Ochoa-Correa, D.; Villa-Ávila, E. (2025). Towards energy efficiency: Innovations in high-frequency converters for renewable energy systems and electric vehicles. *Vehicles*, *7*, 1. https://doi.org/10.3390/vehicles7010001.

© 2025 by the authors. This article is an open access article distributed under the terms and conditions of the Creative Commons Attribution (CC BY) license (http://creativecommons.org/licenses/by/4.0/).